Nuclear Instruments and Methods in Physics Research B 407 (2017) 236–243

Contents lists available at ScienceDirect

Nuclear Instruments and Methods in Physics Research B

journal homepage: www.elsevier.com/locate/nimb

Ionization probabilities of Ne, Ar, Kr, and Xe by proton impact for different initial states and impact energies

C.C. Montanari *, J.E. Miraglia

Instituto de Astronomía y Física del Espacio (CONICET and Universidad de Buenos Aires), Buenos Aires, Argentina
Universidad de Buenos Aires, Facultad de Ciencias Exactas y Naturales, Departamento de Física, 1428 Buenos Aires, Argentina

ARTICLE INFO

Article history:
Received 20 June 2017
Accepted 2 July 2017

Keywords:
Ionization
Impact-parameter
Proton
Rare-gases
CDW-EIS
Born

ABSTRACT

In this contribution we present *ab initio* results for ionization total cross sections, probabilities at zero impact parameter, and impact parameter moments of order +1 and −1 of Ne, Ar, Kr, and Xe by proton impact in an extended energy range from 100 keV up to 10 MeV. The calculations were performed by using the continuum distorted wave eikonal initial state approximation (CDW-EIS) for energies up to 1 MeV, and using the first Born approximation for larger energies. The convergence of the CDW-EIS to the first Born above 1 MeV is clear in the present results. Our inner-shell ionization cross sections are compared with the available experimental data and with the ECPSSR results. We also include in this contribution the values of the ionization probabilities at the origin, and the impact parameter dependence. These values have been employed in multiple ionization calculations showing very good description of the experimental data. Tables of the ionization probabilities are presented, disaggregated for the different initial bound states, considering all the shells for Ne and Ar, the M-N shells of Kr and the N-O shells of Xe.

1. Introduction

Ionization data, involving experimental and theoretical values, has received great attention for a very long time ([1] and references therein). However, current progress of beam characterization methods, atomic analytical techniques such as the so-extended particle induced X-ray emission (PIXE) [2,3], and multiple-purpose simulations for the passage of particles through matter as the Geant4 [4], have aroused new interest and requirements of accurate data and reliable predictions. The probabilities as function of the impact parameter are the seeds to describe the total ionization cross sections of the different shells. But also, these probabilities are the inputs for the multiple ionization calculations in a multinomial combination of the impact parameter probabilities [5]. From the theoretical point of view, these probabilities represent a challenge and a test of the capability of a theory to describe wave functions and interaction potentials. Different approaches have been employed over the years, from the basic first Born approximation, to distorted wave methods, numerical solution of the Schrödinger equation or collective response models [6–11]. Moreover, in very recent works, the ionization probabilities by proton and antiproton impact have been the seeds to obtain multiple ionization cross sections of rare gases by electron and positron impact, with reasonably good results [12,13]. It is worth to note that multiple ionization cross sections are highly dependent on the inner-shell ionization probabilities, which contribute to the final values through Auger-type processes [8,12].

There are different compilations of experimental data for the total ionization cross sections of the K-shell [14,15] and the L-shell [1,16]. One of the most employed models for K and L-shell ionization cross sections is the ECPSSR by Brandt and Lapicki [17,18], of high efficiency and the usual input in PIXE codes [19]. Instead, reliable values of M-shell ionization are scarce [20,21]. This is related to the complexity of the M-X-ray spectra because of the existence of five sub-shells [22].

The goal of the present contribution is to make available *ab initio* CDW-EIS and first Born approximation results for proton impact ionization of different sub-shells of the heaviest rare gases. Presents results are calculated by rigorously solving the radial Schrödinger equation for different angular momenta for both the initial bound and the final continuum states. Thus, we can assure the proper description of the continuum wave function and its mathematical orthogonality to the bound state. These values have already been tested in total [23] and differential [24] ionization cross sections. Also the probabilities as function of the impact

* Corresponding author at: Universidad de Buenos Aires, Facultad de Ciencias Exactas y Naturales, Departamento de Física, 1428 Buenos Aires, Argentina.
E-mail address: mclaudia@iafe.uba.ar (C.C. Montanari).

http://dx.doi.org/10.1016/j.nimb.2017.07.001
0168-583X/

parameter have been employed in multiple ionization calculations [9,12,13,25] with good agreement with the experimental data, even for sextuple ionization of Kr (Xe), where L-shell (M-shell) contribution is decisive. In the following sections we compare the present inner-shell ionization cross sections with the available experimental data, and with the ECPSSR values [17], for the K-shell of Ne, K and L-shells of Ar, L and M-shells of Kr and M and N-shells of Xe. We make available our CDW-EIS values for proton impact energies 0.1–1 MeV, and also the first Born approximation results for proton energies 1–10 MeV, considering the ionization of different sub-shells: Ne (1s, 2s, 2p), Ar (1s,. . ., 3p), Kr (2s,. . ., 4p) and Xe (3s,. . ., 5p). We display tables of the present total ionization cross sections, probabilities at zero impact parameter, and impact parameter moments of order 1 and −1. Atomic units are used throughout this work, except when specifically mentioned.

2. Total ionization cross sections

The total ionization cross section of an electron initially in the *nlm* state, due to the interaction with a heavy projectile of charge Z_P (in this work $Z_P = 1$, proton impact) and impact velocity v, is given by the four-dimension integral

$$\sigma_{nlm} = \frac{(2\pi)^2}{v^2} \int d\vec{k} \int d\vec{\eta} \left| T_{\vec{k},nlm}(\vec{\eta}) \right|^2 \tag{1}$$

where $T_{\vec{k},nlm}(\vec{\eta})$ is the transition matrix as a function of the momentum transferred $\vec{\eta}$ perpendicular to the incident velocity $\vec{v}$, and $\vec{k}$ is the momentum of the emitted electron. For heavy projectiles such as protons, the integration over $\vec{\eta}$ extends to infinity.

If we are interested in high energy collisions, we can resort to the first Born approximation. This is a perturbative method valid at large impact velocities and low projectile charges, with the initial and final wave functions being the unperturbed ones. The first Born transition matrix element is given by

$$T^{Born}_{\vec{k},nlm}(\vec{\eta}) = \frac{1}{(2\pi)^{3/2}} \widetilde{V}_P(p) \int d\vec{r}\ \varphi^*_{\vec{k}}(r)\ \exp(i\ \vec{p}\,.\,\vec{r})\varphi_{nlm}(r). \tag{2}$$

Here $\varphi_{\vec{k}}$ (φ_{nlm}) is the final (initial) continuum (bound) eigenfunction of the target hamiltonian; $\widetilde{V}_P(p) = -\sqrt{2/\pi}\ Z_P/p^2$ is the Fourier transform of the projectile-electron Coulomb potential, and $\vec{p} = \vec{K}_i - \vec{K}_f$ is the momentum transferred, with $\vec{K}_i$ ($\vec{K}_f$) being the initial (final) projectile momentum. The momentum transferred can also be expressed as $\vec{p} = (\vec{\eta}, p_m)$, with p_m being the minimum momentum transfer along the direction of $\vec{v}$, $p_m = (\varepsilon_f - \varepsilon_i)/v$, and ε_i (ε_f) the initial (final) electron energy.

If we are interested in the intermediate energy regime, i.e. proton energies smaller than 1 MeV, we have to improve the calculation of the transition matrix. To that end we resort to the rigorous calculations using the CDW-EIS approximation [23,24]. This model, initially proposed by Crothers and McCann [26], is one of the most reliable approximations to deal with calculations of ionization probabilities in the intermediate to high energy regime [27,28]. Within the CDW-EIS approach the distorted wave functions include the projectile distortion in the initial and final channels. The T-matrix element reads

$$T^{CDW-EIS}_{\vec{k},nlm}(\vec{\eta}) = -\frac{1}{(2\pi)^{3/2}}\ \vec{W}(\vec{p}) \cdot \vec{G}_{\vec{k},nlm}(\vec{p}), \tag{3}$$

with

$$\vec{G}_{\vec{k},nlm}(\vec{p}) = \int d\vec{r}\ \left[\vec{\nabla}\,\varphi_{\vec{k}}(\vec{r})\right]^* e^{i\ \vec{p}\cdot\vec{r}}\ \varphi_{nlm}(\vec{r}), \tag{4}$$

$$\vec{W}(\vec{p}) = N_\xi \int \frac{d\vec{r}}{(2\pi)^{3/2}}\ E^+_{\vec{v}}(\vec{r})\ e^{-i\ \vec{p}\cdot\vec{r}}\ \ \vec{\nabla} F^{-*}_{\vec{v}}(\vec{r}), \tag{5}$$

$$E^+_{\vec{v}}(\vec{r}) = \exp\left[-i\xi \ln(v\ r + \vec{v}\cdot\vec{r})\right], \tag{6}$$

$$F^-_{\vec{v}}(\vec{r}) = {}_1F_1(-i\xi, 1, -iv\ r - i\,\vec{v}\cdot\vec{r}), \tag{7}$$

and

$$N_\xi = \exp(\xi/2)\Gamma(1+i\xi), \tag{8}$$

where $\xi = Z_P/v$, and ${}_1F_1$ is the confluent hypergeometric. In our case, both φ_{nlm} and $\varphi_{\vec{k}}$ are numerical solutions of the same Hamiltonian, therefore fully orthogonal, then the transition matrix $T^{CDW-EIS}_{if}$ does not display prior-post discrepancies.

The initial bound and final continuum radial wave functions were obtained by using the RADIALF code developed by Salvat and co-workers [29]. The number of pivots used to solve the Schrödinger equation rounds a few thousands of points, depending on the number of oscillations of the continuum. The radial integration was performed using the cubic spline technique. The number of angular momenta considered, $l_{\max}$, varied between 8, at very low ejected-electron energies, up to 28, at the largest energies considered. The same number of azimuth angles were required to obtain the fourfold differential cross section (on $\vec{k}$ and $\vec{\eta}$). Each total cross section σ_{nlm} in Eq. (1) was calculated using 35 to 199 momentum transfer values of η to determine a doubly differential cross section, 28 fixed electron angles and around 40 electron energies ($E = k^2/2$), depending on the projectile impact energy.

In the Tables 1–3 we report our results for proton impact total ionization cross sections of Ne, Ar, Kr, and Xe. CDW-EIS values are displayed for impact energies 0.1–1 MeV, and the first Born approximation for 1–10 MeV. A comparison between them is possible at 1 MeV. In all these cases we show separately the contributions of the different *nlm* initial states, raging from the valence shell to two deeper shells.

3. Inner-shell ionization

The total ionization cross sections are determined mainly by the outer target shells. The CDW-EIS and first Born approximation proved to be effective in the description of these total cross sections, as shown in [23]. However, the cross sections for highly ionized targets strongly depend on the inner-shell contributions due to Auger cascade processes. I.e. the ionization of the K-shell of Ar, the L-shell of Kr and the M-shell of Xe are very important to describe the triple to sextuple ionization cross sections at hight impact energies) [25,12].

We test the theoretical values displayed in Tables 1–3, in Figs. 1–4 by comparing with the experimental data available (only available for the K and L-shells) and with the ECPSSR values obtained using the ISICS11 code by Cipolla [30] (we take note of the comments by Smit and Lapicki [31] about this code). To our knowledge, no measurements have been reported for the M-shell ionization of Kr and Xe, or the N-shell ionization of Xe by proton impact.

The K-shell ionization cross section displayed in Fig. 1 shows good agreement with the data. Note that for proton impact energy above 700 keV, the multiple ionization of Ne is sensitive to the K-shell ionization. It contributes directly to multiple ionization via single ionization of one K-shell electron followed by post-collisional electron emission via Auger processes. Similar importance has the L-shell of Ar displayed in Fig. 2. For this shell we include in Fig. 2 the proton impact data compiled by Miranda and Lapicki [1], and the deuteron impact data by Watson and

Table 1
Total ionization cross sections σ_{nlm} of the different sub-shells of Neon and Argon by impact of (0.1–10 MeV) protons. The cross sections for the different *nlm* sub-shells are given by Eq. (1), calculated with the CDW-EIS, Eq. (3), for impact energies 0.1–1 MeV; and with the first Born, Eq. (2), for impact energies 1–10 MeV. To save space, throughout these tables the subindex n replaces the 10^n factor. Units: the energy is in MeV and the cross sections in atomic units.

	Ne												
	CDW-EIS							Born					
E	0.1	0.2	0.3	0.4	0.5	0.7	1	1	2	3	5	7	10
σ_{2p1}	8.17_{-1}	7.96_{-1}	6.86_{-1}	5.95_{-1}	5.25_{-1}	4.26_{-1}	3.36_{-1}	3.41_{-1}	2.04_{-1}	1.49_{-1}	9.93_{-2}	7.55_{-2}	5.63_{-2}
σ_{2p0}	8.79_{-1}	9.03_{-1}	7.72_{-1}	6.59_{-1}	5.71_{-1}	4.52_{-1}	3.46_{-1}	3.44_{-1}	1.99_{-1}	1.43_{-1}	9.35_{-2}	7.09_{-2}	5.19_{-2}
σ_{2s}	2.49_{-1}	2.86_{-1}	2.40_{-1}	2.00_{-1}	1.69_{-1}	1.30_{-1}	9.62_{-2}	9.46_{-2}	5.30_{-2}	3.74_{-2}	2.40_{-2}	1.78_{-2}	1.30_{-2}
σ_{1s}	2.04_{-5}	1.44_{-4}	3.29_{-4}	5.20_{-4}	6.99_{-4}	9.92_{-4}	1.29_{-3}	1.34_{-3}	1.58_{-3}	1.50_{-3}	1.25_{-3}	1.04_{-3}	8.35_{-4}
	Ar												
	CDW-EIS							Born					
E	0.1	0.2	0.3	0.4	0.5	0.7	1	1	2	3	5	7	10
σ_{3p1}	2.86	2.31	1.84	1.53	1.32	1.08	7.85_{-1}	7.98_{-1}	4.54_{-1}	3.24_{-1}	2.21_{-1}	1.56_{-1}	1.16_{-1}
σ_{3p0}	3.52	2.68	2.04	1.65	1.38	1.10	7.79_{-1}	7.85_{-1}	4.32_{-1}	3.04_{-1}	1.94_{-1}	1.52_{-1}	1.05_{-1}
σ_{3s}	6.62_{-1}	5.09_{-1}	3.77_{-1}	2.98_{-1}	2.47_{-1}	1.85_{-1}	1.35_{-1}	1.36_{-1}	7.27_{-2}	5.01_{-2}	3.16_{-2}	2.28_{-2}	1.66_{-2}
σ_{2p1}	2.73_{-3}	7.71_{-3}	1.11_{-2}	1.32_{-2}	1.44_{-2}	1.54_{-2}	1.51_{-2}	1.61_{-2}	1.24_{-2}	9.96_{-3}	7.33_{-3}	5.71_{-3}	4.41_{-3}
σ_{2p0}	2.14_{-3}	6.98_{-3}	1.18_{-2}	1.41_{-2}	1.58_{-2}	1.73_{-2}	1.73_{-2}	1.71_{-2}	1.36_{-2}	1.08_{-2}	7.68_{-3}	5.98_{-3}	4.53_{-3}
σ_{2s}	1.16_{-3}	4.91_{-3}	7.49_{-3}	8.93_{-3}	9.69_{-3}	1.01_{-2}	9.69_{-3}	1.04_{-2}	7.40_{-3}	5.67_{-3}	3.91_{-3}	3.01_{-3}	2.27_{-3}
σ_{1s}	2.08_{-8}	3.52_{-7}	1.41_{-6}	3.35_{-6}	6.07_{-6}	1.33_{-5}	2.62_{-5}	2.73_{-5}	6.86_{-5}	9.58_{-5}	1.20_{-4}	1.24_{-4}	1.19_{-4}

Table 2
Total ionization cross sections σ_{nlm} of Krypton L, M and N shells by 0.1–10 MeV protons. Explanation as in Table 1.

	Kr												
	CDW-EIS							Born					
E	0.1	0.2	0.3	0.4	0.5	0.7	1	1	2	3	5	7	10
σ_{4p1}	3.36	2.51	1.94	1.58	1.35	1.04	7.77_{-1}	8.01_{-1}	4.38_{-1}	3.09_{-1}	1.98_{-1}	1.47_{-1}	1.07_{-1}
σ_{4p0}	4.48	2.91	2.12	1.76	1.38	1.03	7.53_{-1}	7.70_{-1}	4.24_{-1}	2.95_{-1}	1.79_{-1}	1.32_{-1}	9.52_{-2}
σ_{4s}	9.92_{-1}	7.03_{-1}	5.09_{-1}	3.96_{-1}	3.24_{-1}	2.38_{-1}	1.70_{-1}	1.71_{-1}	8.80_{-2}	5.95_{-2}	3.63_{-2}	2.62_{-2}	1.88_{-2}
σ_{3d2}	1.98_{-2}	3.53_{-2}	4.20_{-2}	4.45_{-2}	4.50_{-2}	4.37_{-2}	4.01_{-2}	4.25_{-2}	3.07_{-2}	2.43_{-2}	1.75_{-2}	1.39_{-2}	1.08_{-2}
σ_{3d1}	2.42_{-2}	4.13_{-2}	4.85_{-2}	5.14_{-2}	5.20_{-2}	5.04_{-2}	4.59_{-2}	4.65_{-2}	3.31_{-2}	2.57_{-2}	1.80_{-2}	1.40_{-2}	1.06_{-2}
σ_{3d0}	2.65_{-2}	4.81_{-2}	5.65_{-2}	5.88_{-2}	5.86_{-2}	5.54_{-2}	4.93_{-2}	4.79_{-2}	3.37_{-2}	2.61_{-2}	1.80_{-2}	1.39_{-2}	1.05_{-2}
σ_{3p1}	3.36_{-3}	9.02_{-3}	1.24_{-2}	1.42_{-2}	1.50_{-2}	1.52_{-2}	1.41_{-2}	1.51_{-2}	1.04_{-2}	7.96_{-3}	5.48_{-3}	4.23_{-3}	3.19_{-3}
σ_{3p0}	3.38_{-3}	9.92_{-3}	1.48_{-2}	1.70_{-2}	1.77_{-2}	1.74_{-2}	1.59_{-2}	1.63_{-2}	1.13_{-2}	8.46_{-3}	5.65_{-3}	4.28_{-3}	3.16_{-3}
σ_{3s}	1.40_{-3}	5.63_{-3}	8.22_{-3}	9.44_{-3}	1.00_{-2}	1.02_{-2}	9.62_{-3}	1.03_{-2}	7.10_{-3}	5.38_{-3}	3.65_{-3}	2.79_{-3}	2.09_{-3}
σ_{2p1}	5.88_{-7}	7.13_{-6}	2.28_{-5}	4.59_{-5}	7.36_{-5}	1.33_{-4}	2.14_{-4}	2.31_{-4}	3.71_{-4}	4.13_{-4}	4.13_{-4}	3.80_{-4}	3.31_{-4}
σ_{2p0}	1.80_{-6}	1.16_{-5}	2.72_{-5}	4.59_{-5}	6.54_{-5}	1.03_{-4}	1.58_{-4}	1.80_{-4}	3.28_{-4}	4.00_{-4}	4.33_{-4}	4.12_{-4}	3.64_{-4}
σ_{2s}	2.74_{-7}	1.40_{-6}	7.86_{-6}	2.21_{-5}	4.30_{-5}	9.70_{-5}	1.83_{-4}	1.90_{-4}	3.38_{-4}	3.73_{-4}	3.50_{-4}	3.09_{-4}	2.56_{-4}

Table 3
Total ionization cross sections σ_{nlm} of Xenon M, N and O shells by 0.1–10 MeV protons. Explanation as in Table 1.

	Xe												
	CDW-EIS							Born					
E	0.1	0.2	0.3	0.4	0.5	0.7	1	1	2	3	5	7	10
σ_{5p1}	5.09	3.52	2.67	2.16	1.82	1.40	1.05	1.06	5.91_{-1}	4.18_{-1}	2.68_{-1}	2.08_{-1}	1.46_{-1}
σ_{5p0}	6.46	4.07	2.93	2.29	1.89	1.41	1.03	1.03	5.53_{-1}	3.85_{-1}	2.42_{-1}	1.80_{-1}	1.29_{-1}
σ_{5s}	1.72	1.05	7.37_{-1}	5.67_{-1}	4.61_{-1}	3.36_{-1}	2.39_{-1}	2.39_{-1}	1.22_{-1}	8.23_{-2}	5.00_{-2}	3.60_{-2}	2.54_{-2}
σ_{4d2}	1.80_{-1}	2.35_{-1}	2.33_{-1}	2.20_{-1}	2.06_{-1}	1.79_{-1}	1.50_{-1}	1.55_{-1}	9.96_{-2}	7.52_{-2}	5.17_{-2}	3.99_{-2}	3.03_{-2}
σ_{4d1}	2.12_{-1}	2.77_{-1}	2.72_{-1}	2.54_{-1}	2.35_{-1}	2.00_{-1}	1.63_{-1}	1.67_{-1}	1.03_{-1}	7.59_{-2}	5.08_{-2}	3.87_{-2}	2.90_{-2}
σ_{4d0}	2.16_{-1}	3.01_{-1}	2.99_{-1}	2.77_{-1}	2.53_{-1}	2.12_{-1}	1.70_{-1}	1.72_{-1}	1.04_{-1}	7.59_{-2}	5.03_{-2}	3.81_{-2}	2.83_{-2}
σ_{4p1}	1.67_{-2}	2.77_{-2}	2.99_{-2}	2.96_{-2}	2.84_{-2}	2.54_{-2}	2.12_{-2}	2.21_{-2}	1.37_{-2}	1.00_{-2}	6.65_{-3}	5.02_{-3}	3.71_{-3}
σ_{4p0}	1.33_{-2}	3.67_{-2}	4.21_{-2}	3.99_{-2}	3.65_{-2}	3.05_{-2}	2.46_{-2}	2.49_{-2}	1.45_{-2}	1.02_{-2}	6.44_{-3}	4.73_{-3}	3.39_{-3}
σ_{4s}	9.35_{-3}	1.92_{-2}	1.98_{-2}	1.93_{-2}	1.86_{-2}	1.71_{-2}	1.48_{-2}	1.51_{-2}	9.48_{-3}	6.96_{-3}	4.60_{-3}	3.47_{-3}	2.56_{-3}
σ_{3d2}	6.01_{-5}	3.14_{-4}	6.33_{-4}	9.33_{-4}	1.19_{-3}	1.57_{-3}	1.89_{-3}	2.00_{-3}	2.20_{-3}	2.09_{-3}	1.78_{-3}	1.54_{-3}	1.28_{-3}
σ_{3d1}	7.22_{-5}	2.59_{-4}	4.64_{-4}	6.62_{-4}	8.53_{-4}	1.22_{-3}	1.68_{-3}	1.83_{-3}	2.31_{-3}	2.30_{-3}	2.00_{-3}	1.71_{-3}	1.40_{-3}
σ_{3d0}	7.46_{-5}	2.62_{-4}	4.32_{-4}	5.94_{-4}	7.67_{-4}	1.12_{-3}	1.56_{-3}	1.73_{-3}	2.34_{-3}	2.36_{-3}	2.08_{-3}	1.78_{-3}	1.44_{-3}
σ_{3p1}	6.23_{-6}	7.72_{-5}	2.37_{-4}	4.40_{-4}	6.48_{-4}	9.99_{-4}	1.31_{-3}	1.27_{-3}	1.42_{-3}	1.30_{-3}	1.04_{-3}	8.53_{-4}	6.76_{-4}
σ_{3p0}	1.73_{-5}	9.49_{-5}	2.02_{-4}	3.31_{-4}	4.63_{-4}	7.04_{-4}	1.03_{-3}	1.08_{-3}	1.42_{-3}	1.38_{-3}	1.14_{-3}	9.39_{-4}	7.36_{-4}
σ_{3s}	3.37_{-6}	2.55_{-5}	1.13_{-4}	2.53_{-4}	4.17_{-4}	7.38_{-4}	1.06_{-3}	9.86_{-4}	1.14_{-3}	1.04_{-3}	8.14_{-4}	6.60_{-4}	5.15_{-4}

Toburen [44]. For the ionization of Ar K-shell the agreement with the experiments and the ECPSSR is very good. For L-shell ionization, our description differs from the ECPSSR one, while the experimental data seems to be in between both curves.

Perhaps the most interesting feature is displayed in Fig. 3 for Kr. For L-shell ionization the agreement of the present results with the measurements by Winters *et al.* [36] and Czuchlewski *et al.* [37], and with the ECPSSR is very good. However, for M-shell ionization the situation is different: we got a clear discrepancy with the ECPSSR results [30] and no experimental data is available. Present M-shell ionization probabilities of Kr have already been employed in multiple ionization calculations with very good agreement with

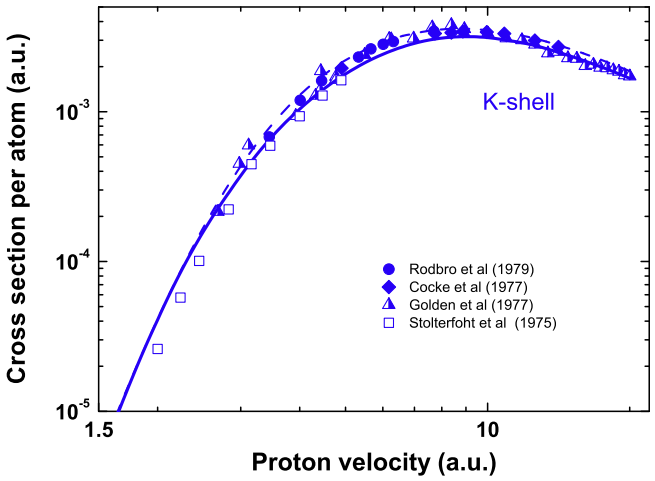

Fig. 1. K-shell ionization cross section of Ne by proton impact. Curves: solid line, present results displayed in Table 1; dashed line, ECPSSR [17,30]. Symbols: experimental data by Rodbro *et al.* [32], Cocke *et al.* [33], Golden *et al.* [34], and Stolterfoht *et al.* [35].

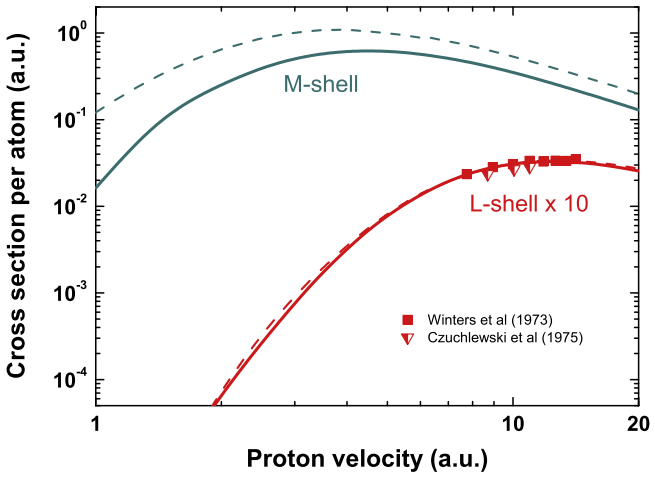

Fig. 3. L and M-shell ionization cross sections of Kr by proton impact. Curves: solid line, present results displayed in Table 2; dashed line, ECPSSR. Symbols: experimental data for L-shell ionization by Winters *et al.* [36], and by Czuchlewski *et al.* [37].

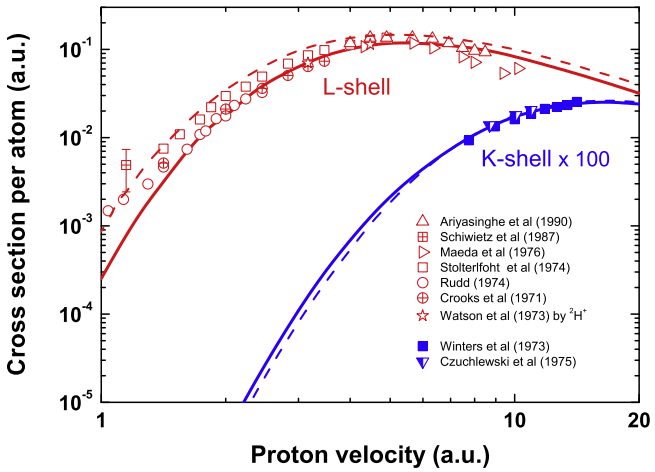

Fig. 2. K and L-shell ionization cross sections of Ar by proton impact. Curves: solid line, present results displayed in Table 1; dashed line, ECPSSR [17,30]. Symbols: K-shell experimental data by Winters *et al.* [36], and by Czuchlewski *et al.* [37]; L-shell experimental data by Ariyasinghe *et al.* [38], Schiwietz *et al.* [39], Maeda et al. [40], Stolterfoht *et al.* [41], Rudd [42], Crooks and Rudd [43], and Watson and Toburen [44] (deuteron impact).

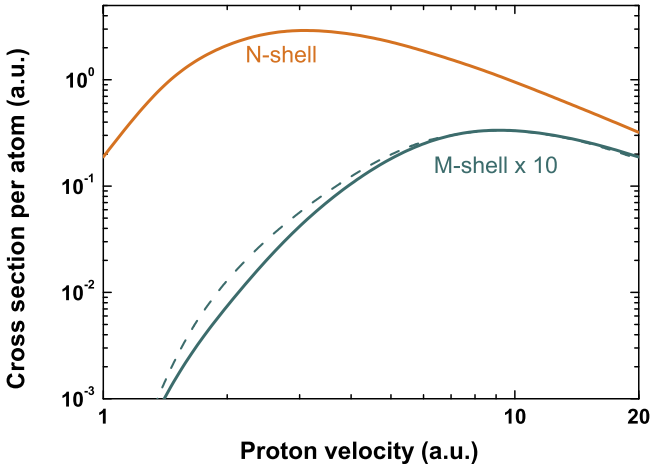

Fig. 4. M and N-shell ionization cross sections of Xe by proton impact. Curves: solid line, present results displayed in Table 3; dashed line, ECPSSR.

the experimental data [9,25]. In triple and quadruple ionization of Kr at high energies the M-shell ionization plays a mayor role due to single ionization followed by Auger emission of 2 or more electrons. This is also a test of the present results validity.

Finally, in Fig. 4 we display the M and N-shell ionization cross sections of Xe. Good agreement with ECPSSR is observed for the M-shell ionization at high energies, and a clear difference below 500 keV. The M-shell of Xe is very important in quintuple and sextuple ionization above 1 MeV [25,12], which is the region where both calculations agree well.

4. Ionization probabilities as a function of the impact parameter

The transition amplitude $a_{\vec{k},nlm}(\vec{b})$ as a function of the impact parameter $\vec{b}$ is defined with the help of the bi-dimensional Fourier transform

$$a_{k^{\rightarrow},nlm}(\vec{b}) = \int d\vec{\eta}\,\frac{\exp(i\vec{b}\cdot\vec{\eta})}{2\pi}\; T_{k^{\rightarrow},nlm}(\vec{\eta}). \tag{9}$$

with the probability being $P_{\vec{k},nlm}(\vec{b}) = \left|a_{\vec{k},nlm}(\vec{b})\right|^2$. To solve Eq. (9) we expanded

$$T_{k^{\rightarrow},nlm}(\vec{\eta}) = \sum_{\mu=-M}^{M} i^{\mu}\frac{\exp(i\mu\ \varphi_{\eta})}{\sqrt{2\pi}}\; T^{(\mu)}_{k^{\rightarrow},nlm}(\eta). \tag{10}$$

where $\vec{\eta} = \{\eta, \varphi_{\eta}\}$. We integrated numerically the T-matrix elements for different angular momentum and added them appropriately. To be consistent, the maximum value M was considered to be the maximum angular momenta used to solve the Schrödinger equation. Special care should be taken to obtain $T^{(\mu)}_{\vec{k},nlm}(\eta)$ (see details in [9]). For practical purposes all these $T^{(\mu)}_{\vec{k},nlm}(\eta)$ values were stored in a large table of $(2\times 8+1)$ to $(2\times 28+1)$ values of μ, around 70 values of η, 28 electron angles Ω, and between 33 to 45 values of E, which are available upon request.

Afterwards, Eq. (9) can be written as

$$a_{k^{\rightarrow},nlm}(\vec{b}) = \sum_{\mu=-M}^{M} i^{\mu} \frac{\exp(i\mu\ \varphi_{\eta})}{\sqrt{2\pi}}\ a^{(\mu)}_{k^{\rightarrow},nlm}(b), \tag{11}$$

with

$$a^{(\mu)}_{k^{\rightarrow},nlm}(b) = i^{-\mu} \int_0^{\infty} d\eta\ \eta\ \ J_{\mu}(b\ \eta)\ T^{(\mu)}_{k^{\rightarrow},nlm}(\eta), \tag{12}$$

and with $J_{\mu}(b\ \eta)$ being the cylindrical Bessel function. Then the total ionization probability as a function of the impact parameter is obtained after integrating in the ejection electron space

$$P_{nlm}(\vec{b}) = \frac{1}{2\pi} \sum_{m=-M}^{M} \int d\vec{k}\ \left| a^{(\mu)}_{k^{\rightarrow},nlm}(b) \right|^2. \tag{13}$$

It is always convenient to re-calculate the total cross section as $\sigma_{nlm} = \int d\vec{b}\ \ P_{nlm}(\vec{b})$ to check the procedure.

These impact parameter dependent probabilities are very important because they are the seeds to get the different multiple ionization ones by introducing them in the multinomial expansion [6,8]. For multiple processes the probability at small impact parameters is very important. In Tables 4–6 we display the geometrical factor $P_{nlm}(0)$ for the four rare gases, considering the different sub-shells and impact energies.

Table 4
Ionization probabilities at zero impact parameter, $P_{nlm}(b=0)$, of Neon and Argon different sub-shells by 0.1–10 MeV protons. The ionization probabilities are given by Eq. (13), and they were calculated with the CDW-EIS approximation for impact energies 0.1–1 MeV, and with the first Born approximation for impact energies 1–10 MeV. To save space, throughout these tables the subindex n replaces the 10^n factor.

	Ne												
	CDW-EIS							Born					
E	0.1	0.2	0.3	0.4	0.5	0.7	1	1	2	3	5	7	10
2*p*1	8.50_{-2}	8.17_{-2}	6.97_{-2}	5.98_{-2}	5.20_{-2}	4.11_{-2}	3.10_{-2}	3.40_{-2}	1.75_{-2}	1.18_{-2}	7.06_{-3}	5.03_{-3}	3.51_{-3}
2*p*0	2.19_{-1}	1.92_{-1}	1.51_{-1}	1.23_{-1}	1.02_{-1}	7.60_{-2}	5.38_{-2}	5.80_{-2}	2.73_{-2}	1.77_{-2}	1.02_{-2}	7.17_{-3}	4.94_{-3}
2*s*	3.97_{-2}	4.47_{-2}	4.27_{-2}	3.97_{-2}	3.67_{-2}	3.18_{-2}	2.62_{-2}	2.63_{-2}	1.60_{-2}	1.14_{-2}	7.11_{-3}	5.15_{-3}	3.63_{-3}
1*s*	6.78_{-4}	3.15_{-3}	5.81_{-3}	7.87_{-3}	9.47_{-3}	1.13_{-2}	1.22_{-2}	1.28_{-2}	1.18_{-2}	1.01_{-2}	7.32_{-3}	5.60_{-3}	4.09_{-3}
	Ar												
	CDW-EIS							Born					
E	0.1	0.2	0.3	0.4	0.5	0.7	1	1	2	3	5	7	10
3*p*1	9.51_{-2}	6.78_{-2}	5.21_{-2}	4.23_{-2}	3.56_{-2}	2.72_{-2}	2.02_{-2}	2.09_{-2}	1.12_{-2}	7.62_{-3}	4.66_{-3}	3.36_{-3}	2.36_{-3}
3*p*0	2.85_{-1}	1.77_{-1}	1.28_{-1}	1.01_{-1}	8.38_{-2}	6.25_{-2}	4.52_{-2}	4.53_{-2}	2.32_{-2}	1.54_{-2}	9.16_{-3}	6.49_{-3}	4.55_{-3}
3*s*	5.67_{-2}	5.92_{-2}	4.99_{-2}	4.11_{-2}	3.44_{-2}	2.57_{-2}	1.87_{-2}	1.93_{-2}	1.03_{-2}	7.08_{-3}	4.41_{-3}	3.21_{-3}	2.27_{-3}
2*p*1	4.02_{-3}	1.09_{-2}	1.47_{-2}	1.64_{-2}	1.71_{-2}	1.71_{-2}	1.57_{-2}	1.60_{-2}	1.08_{-2}	7.96_{-3}	5.17_{-3}	3.81_{-3}	2.70_{-3}
2*p*0	8.58_{-3}	3.02_{-2}	4.51_{-2}	5.36_{-2}	5.72_{-2}	5.73_{-2}	5.12_{-2}	4.56_{-2}	2.74_{-2}	1.87_{-2}	1.10_{-2}	7.65_{-3}	5.19_{-3}
2*s*	3.83_{-3}	1.08_{-2}	1.26_{-2}	1.22_{-2}	1.12_{-2}	9.34_{-3}	7.96_{-3}	8.42_{-3}	7.27_{-3}	6.46_{-3}	5.00_{-3}	3.98_{-3}	3.01_{-3}
1*s*	8.15_{-6}	7.81_{-5}	2.21_{-4}	4.09_{-4}	6.29_{-4}	1.12_{-3}	1.80_{-3}	1.91_{-3}	3.23_{-3}	3.68_{-3}	3.76_{-3}	3.58_{-3}	3.11_{-3}

Table 5
Ionization probabilities at zero impact parameter, $P_{nlm}(b=0)$, of Krypton M and N shells by 0.1–10 MeV protons. Explanation as in Table 4.

	Kr												
	CDW-EIS							Born					
E	0.1	0.2	0.3	0.4	0.5	0.7	1	1	2	3	5	7	10
4*p*1	1.04_{-1}	6.64_{-2}	4.88_{-2}	3.86_{-2}	3.19_{-2}	2.38_{-2}	1.72_{-2}	1.74_{-2}	9.08_{-3}	6.17_{-3}	3.77_{-3}	2.72_{-3}	1.92_{-3}
4*p*0	3.57_{-1}	1.89_{-1}	1.32_{-1}	1.02_{-1}	8.22_{-2}	5.91_{-2}	4.10_{-2}	4.11_{-2}	2.03_{-2}	1.36_{-2}	8.19_{-3}	5.86_{-3}	4.12_{-3}
4*s*	5.62_{-2}	6.31_{-2}	4.99_{-2}	3.98_{-2}	3.29_{-2}	2.48_{-2}	1.84_{-2}	1.84_{-2}	1.01_{-2}	6.90_{-3}	4.21_{-3}	3.04_{-3}	2.15_{-3}
3*d*2	1.31_{-2}	2.06_{-2}	2.29_{-2}	2.32_{-2}	2.24_{-2}	2.03_{-2}	1.73_{-2}	1.79_{-2}	1.11_{-2}	7.99_{-3}	5.11_{-3}	3.75_{-3}	2.67_{-3}
3*d*1	2.50_{-2}	4.16_{-2}	4.66_{-2}	4.67_{-2}	4.48_{-2}	3.97_{-2}	3.25_{-2}	3.13_{-2}	1.82_{-2}	1.25_{-2}	7.45_{-3}	5.25_{-3}	3.61_{-3}
3*d*0	4.67_{-2}	8.28_{-2}	9.40_{-2}	9.46_{-2}	9.07_{-2}	7.88_{-2}	6.24_{-2}	5.57_{-2}	2.94_{-2}	1.93_{-2}	1.10_{-2}	7.60_{-3}	5.15_{-3}
3*p*1	2.94_{-3}	5.69_{-3}	6.65_{-3}	6.77_{-3}	6.58_{-3}	6.01_{-3}	5.33_{-3}	5.49_{-3}	4.40_{-3}	3.70_{-3}	2.82_{-3}	2.27_{-3}	1.75_{-3}
3*p*0	9.69_{-3}	2.44_{-2}	3.15_{-2}	3.24_{-2}	3.04_{-2}	2.50_{-2}	1.88_{-2}	1.64_{-2}	1.22_{-2}	1.05_{-2}	7.89_{-3}	6.13_{-3}	4.51_{-3}
3*s*	2.53_{-3}	6.50_{-3}	7.52_{-3}	7.30_{-3}	7.16_{-3}	7.46_{-3}	8.23_{-3}	8.67_{-3}	6.32_{-3}	4.55_{-3}	2.86_{-3}	2.13_{-3}	1.59_{-3}

Table 6
Ionization probabilities at zero impact parameter, $P_{nlm}(b=0)$, of Xenon N and O shells by 0.1–10 MeV protons. Explanation as in Table 4.

	Xe												
	CDW-EIS							Born					
E	0.1	0.2	0.3	0.4	0.5	0.7	1	1	2	3	5	7	10
5*p*1	9.85_{-2}	6.71_{-2}	4.91_{-2}	3.85_{-2}	3.17_{-2}	2.34_{-2}	1.69_{-2}	1.70_{-2}	8.86_{-3}	6.02_{-3}	3.68_{-3}	2.66_{-3}	1.88_{-3}
5*p*0	3.56_{-1}	2.19_{-1}	1.48_{-1}	1.08_{-1}	8.49_{-2}	5.97_{-2}	4.19_{-2}	4.23_{-2}	2.12_{-2}	1.41_{-2}	8.65_{-3}	6.06_{-3}	4.16_{-3}
5*s*	9.14_{-2}	5.46_{-2}	4.16_{-2}	3.54_{-2}	3.12_{-2}	2.48_{-2}	1.87_{-2}	1.86_{-2}	9.89_{-3}	6.81_{-3}	4.20_{-3}	3.02_{-3}	2.12_{-3}
4*d*2	3.70_{-2}	3.48_{-2}	2.95_{-2}	2.53_{-2}	2.21_{-2}	1.77_{-2}	1.36_{-2}	1.39_{-2}	8.14_{-3}	5.83_{-3}	3.75_{-3}	2.78_{-3}	2.00_{-3}
4*d*1	1.09_{-1}	9.76_{-2}	7.55_{-2}	6.00_{-2}	4.90_{-2}	3.53_{-2}	2.48_{-2}	2.40_{-2}	1.31_{-2}	9.26_{-3}	5.84_{-3}	4.24_{-3}	2.99_{-3}
4*d*0	2.02_{-1}	1.96_{-1}	1.59_{-1}	1.24_{-1}	9.88_{-2}	6.83_{-2}	4.54_{-2}	4.03_{-2}	2.32_{-2}	1.73_{-2}	1.11_{-2}	8.00_{-3}	5.47_{-3}
4*p*1	5.08_{-3}	7.47_{-3}	7.32_{-3}	6.88_{-3}	6.53_{-3}	6.02_{-3}	5.46_{-3}	5.64_{-3}	4.03_{-3}	3.11_{-3}	2.16_{-3}	1.68_{-3}	1.27_{-3}
4*p*0	2.32_{-2}	3.96_{-2}	3.65_{-2}	3.10_{-2}	2.69_{-2}	2.25_{-2}	2.11_{-2}	2.10_{-2}	1.30_{-2}	8.74_{-3}	5.30_{-3}	3.91_{-3}	2.85_{-3}
4*s*	5.46_{-3}	8.71_{-3}	9.12_{-3}	9.87_{-3}	1.04_{-2}	1.07_{-2}	8.99_{-3}	7.74_{-3}	4.79_{-3}	3.79_{-3}	2.66_{-3}	2.01_{-3}	1.45_{-3}

Table 7
Mean radii $\langle r_{nl} \rangle$ of the atomic *nl* sub-shells of Ne, Ar, Kr and Xe (in atomic units).

Ne	Ar	Kr	Xe
$\langle r_{2p} \rangle = 0.9653$	$\langle r_{3p} \rangle = 1.6629$	$\langle r_{4p} \rangle = 1.9516$	$\langle r_{5p} \rangle = 2.3380$
$\langle r_{2s} \rangle = 0.8921$	$\langle r_{3s} \rangle = 1.4222$	$\langle r_{4s} \rangle = 1.6294$	$\langle r_{5s} \rangle = 1.9810$
$\langle r_{1s} \rangle = 0.1576$	$\langle r_{2p} \rangle = 0.3753$	$\langle r_{3d} \rangle = 0.5509$	$\langle r_{4d} \rangle = 0.8704$
	$\langle r_{2s} \rangle = 0.4123$	$\langle r_{3p} \rangle = 0.5426$	$\langle r_{4p} \rangle = 0.7770$
	$\langle r_{1s} \rangle = 0.0861$	$\langle r_{3s} \rangle = 0.5378$	$\langle r_{4s} \rangle = 0.7453$

5. Impact parameter moments

The impact parameter moments concerning each sub-shell ionization are very interesting parameters of the collision. They are defined as

$$\left\langle b^{J}_{nlm} \right\rangle = \frac{1}{\sigma_{nlm}} \int d\vec{b}\; P_{nlm}(\vec{b}) \left(\frac{b}{\langle r_{nl} \rangle} \right)^{J}. \tag{14}$$

To bring these moments to unity, we have normalized to $\langle r_{nl} \rangle$, the mean radius of the initial atomic state as given in Table 7.

Table 8
Impact parameter moment $\left\langle b^{-1}_{nlm} \right\rangle$, given by Eq. (14), for proton in Ne and Ar using the CDW-EIS and the first Born approximations. The values are normalized to the inverse of the mean radius of each sub-shell, $\langle r_{nl} \rangle^{-1}$, given in Table 7. To save space, throughout these tables the subindex n replaces the 10^n factor. The energy is expressed in MeV.

	Ne												
	CDW-EIS							Born					
E	0.1	0.2	0.3	0.4	0.5	0.7	1	1	2	3	5	7	10
2p1	9.15_{-1}	9.17_{-1}	9.08_{-1}	8.95_{-1}	8.82_{-1}	8.57_{-1}	8.26_{-1}	8.36_{-1}	7.58_{-1}	7.16_{-1}	6.65_{-1}	6.35_{-1}	6.05_{-1}
2p0	1.34	1.23	1.18	1.15	1.11	1.07	1.01	1.02	8.97_{-1}	8.37_{-1}	7.68_{-1}	7.29_{-1}	6.91_{-1}
2s	1.19	1.17	1.20	1.23	1.25	1.29	1.31	1.32	1.31	1.29	1.25	1.23	1.19
1s	2.78	2.26	2.02	1.86	1.76	1.60	1.45	1.46	1.28	1.20	1.12	1.06	1.01
	Ar												
	CDW-EIS							Born					
E	0.1	0.2	0.3	0.4	0.5	0.7	1	1	2	3	5	7	10
3p1	1.02	9.76_{-1}	9.48_{-1}	9.25_{-1}	9.05_{-1}	8.76_{-1}	8.45_{-1}	8.53_{-1}	7.90_{-1}	7.60_{-1}	7.22_{-1}	7.03_{-1}	6.85_{-1}
3p0	1.39	1.29	1.24	1.20	1.17	1.13	1.08	1.08	9.93_{-1}	9.50_{-1}	9.00_{-1}	8.75_{-1}	8.56_{-1}
3s	1.37	1.48	1.55	1.57	1.58	1.59	1.59	1.60	1.58	1.56	1.53	1.51	1.48
2p1	1.60	1.45	1.37	1.31	1.26	1.21	1.16	1.16	1.07	1.02	9.60_{-1}	9.18_{-1}	8.73_{-1}
2p0	2.27	2.32	2.21	2.13	2.06	1.94	1.80	1.73	1.48	1.36	1.23	1.15	1.08
2s	2.29	1.90	1.68	1.53	1.43	1.31	1.25	1.26	1.27	1.29	1.30	1.29	1.27
1s	3.38	3.17	2.81	2.58	2.44	2.22	2.02	2.03	1.68	1.53	1.38	1.31	1.23

Table 9
Impact parameter moment $\left\langle b^{-1}_{nlm} \right\rangle$, given by Eq. (14), for proton in Kr using the CDW-EIS and the first Born approximations. Explanation as in Table 8.

	Kr												
	CDW-EIS							Born					
E	0.1	0.2	0.3	0.4	0.5	0.7	1	1	2	3	5	7	10
4p1	1.15	1.09	1.06	1.03	1.01	9.83_{-1}	9.53_{-1}	9.47_{-1}	8.88_{-1}	8.55_{-1}	8.15_{-1}	7.91_{-1}	7.68_{-1}
4p0	1.62	1.48	1.42	1.38	1.35	1.31	1.26	1.25	1.16	1.12	1.06	1.03	9.99_{-1}
4s	1.35	1.50	1.55	1.58	1.59	1.61	1.63	1.62	1.63	1.63	1.62	1.62	1.61
3d2	1.46	1.31	1.24	1.20	1.17	1.12	1.08	1.07	9.92_{-1}	9.43_{-1}	8.81_{-1}	8.40_{-1}	7.99_{-1}
3d1	1.77	1.69	1.62	1.55	1.49	1.41	1.33	1.30	1.17	1.09	9.99_{-1}	9.44_{-1}	8.89_{-1}
3d0	2.14	2.10	2.04	1.97	1.90	1.79	1.65	1.57	1.34	1.23	1.11	1.04	9.75_{-1}
3p1	1.74	1.51	1.38	1.29	1.24	1.18	1.15	1.15	1.15	1.15	1.16	1.15	1.14
3p0	2.72	2.50	2.34	2.22	2.10	1.93	1.76	1.69	1.64	1.65	1.66	1.64	1.61
3s	2.29	1.90	1.70	1.56	1.49	1.44	1.46	1.44	1.45	1.44	1.41	1.39	1.36

Table 10
Impact parameter moment $\left\langle b^{-1}_{nlm} \right\rangle$, given by Eq. (14), for proton in Xenon using the CDW-EIS and the first Born approximations. Explanation as in Table 8.

	Xe												
	CDW-EIS							Born					
E	0.1	0.2	0.3	0.4	0.5	0.7	1	1	2	3	5	7	10
5p1	1.15	1.11	1.07	1.05	1.03	9.99_{-1}	9.68_{-1}	9.72_{-1}	9.13_{-1}	8.84_{-1}	8.52_{-1}	8.36_{-1}	8.21_{-1}
5p0	1.62	1.55	1.49	1.44	1.40	1.35	1.30	1.31	1.22	1.18	1.15	1.12	1.10
5s	1.48	1.51	1.55	1.59	1.62	1.65	1.68	1.68	1.70	1.71	1.70	1.70	1.69
4d2	1.29	1.14	1.08	1.03	1.00	9.60_{-1}	9.18_{-1}	9.22_{-1}	8.46_{-1}	8.04_{-1}	7.54_{-1}	7.22_{-1}	6.90_{-1}
4d1	1.83	1.56	1.41	1.32	1.25	1.17	1.09	1.08	9.75_{-1}	9.20_{-1}	8.56_{-1}	8.16_{-1}	7.76_{-1}
4d0	2.35	1.97	1.78	1.64	1.54	1.40	1.28	1.25	1.12	1.06	9.83_{-1}	9.33_{-1}	8.82_{-1}
4p1	1.64	1.51	1.41	1.35	1.32	1.30	1.31	1.32	1.35	1.36	1.36	1.35	1.34
4p0	3.02	2.44	2.23	2.12	2.05	2.00	2.05	2.02	2.06	2.04	2.00	1.98	1.95
4s	1.98	1.79	1.71	1.69	1.69	1.73	1.73	1.65	1.63	1.64	1.62	1.60	1.57

Table 11
Impact parameter moment $\left\langle b^1_{nlm} \right\rangle$ for proton in Neon and Argon using the CDW-EIS and the first Born approximations. Explanation as in Table 8.

	Ne												
	CDW-EIS							Born					
E	0.1	0.2	0.3	0.4	0.5	0.7	1	1	2	3	5	7	10
2p1	1.85	1.91	2.00	2.09	2.17	2.33	2.53	2.53	3.06	3.44	4.03	4.49	5.05
2p0	1.42	1.58	1.69	1.80	1.90	2.08	2.31	2.33	2.92	3.35	4.01	4.51	5.11
2s	1.30	1.34	1.35	1.36	1.38	1.41	1.45	1.45	1.59	1.70	1.87	2.01	2.19
1s	6.02_{-1}	7.33_{-1}	8.24_{-1}	9.00_{-1}	9.60_{-1}	1.06	1.18	1.18	1.37	1.47	1.62	1.73	1.86
	Ar												
	CDW-EIS							Born					
E	0.1	0.2	0.3	0.4	0.5	0.7	1	1	2	3	5	7	10
3p1	1.55	1.67	1.79	1.90	2.00	2.16	2.36	2.35	2.82	3.06	3.46	3.68	3.88
3p0	1.28	1.44	1.58	1.70	1.81	2.00	2.23	2.22	2.74	3.01	3.44	3.66	3.87
3s	1.13	1.10	1.08	1.08	1.08	1.09	1.11	1.10	1.17	1.24	1.34	1.42	1.53
2p1	9.38_{-1}	1.09	1.18	1.25	1.30	1.36	1.43	1.42	1.58	1.70	1.90	2.05	2.25
2p0	7.55_{-1}	7.62_{-1}	8.01_{-1}	8.43_{-1}	8.88_{-1}	9.67_{-1}	1.07	1.08	1.30	1.45	1.68	1.85	2.07
2s	6.96_{-1}	8.39_{-1}	9.50_{-1}	1.03	1.10	1.11	1.23	1.21	1.28	1.32	1.40	1.47	1.55
1s	3.29_{-1}	4.40_{-1}	5.20_{-1}	5.83_{-1}	6.31_{-1}	7.02_{-1}	7.83_{-1}	7.82_{-1}	9.69_{-1}	1.08	1.22	1.30	1.39

Table 12
Impact parameter moment $\left\langle b^1_{nlm} \right\rangle$ for proton in Kr using the CDW-EIS and the first Born approximations. Explanation as in Table 8.

	Kr												
	CDW-EIS							Born					
E	0.1	0.2	0.3	0.4	0.5	0.7	1	1	2	3	5	7	10
4p1	1.38	1.48	1.58	1.66	1.73	1.86	2.01	2.03	2.44	2.74	3.18	3.49	3.84
4p0	1.12	1.27	1.38	1.48	1.56	1.71	1.88	1.91	2.36	2.69	3.18	3.53	3.90
4s	1.10	1.07	1.05	1.04	1.04	1.04	1.04	1.05	1.07	1.09	1.12	1.16	1.20
3d2	1.15	1.31	1.38	1.43	1.47	1.53	1.60	1.64	1.85	2.00	2.25	2.46	2.70
3d1	9.59_{-1}	1.02	1.09	1.16	1.21	1.29	1.39	1.44	1.68	1.86	2.15	2.37	2.64
3d0	8.46_{-1}	8.86_{-1}	9.41_{-1}	9.99_{-1}	1.05	1.15	1.26	1.34	1.62	1.82	2.12	2.35	2.63
3p1	8.33_{-1}	9.85_{-1}	1.09	1.16	1.21	1.26	1.29	1.46	1.54	1.58	1.65	1.71	1.80
3p0	6.43_{-1}	7.03_{-1}	7.41_{-1}	7.78_{-1}	8.18_{-1}	8.90_{-1}	9.64_{-1}	1.19	1.33	1.42	1.55	1.64	1.75
3s	6.69_{-1}	7.99_{-1}	9.01_{-1}	9.80_{-1}	1.03	1.09	1.11	1.09	1.13	1.16	1.21	1.26	1.33

Table 13
Impact parameter moment $\left\langle b^1_{nlm} \right\rangle$ for proton in Xe using the CDW-EIS and the first Born approximations. Explanation as in Table 8.

	Xe												
	CDW-EIS							Born					
E	0.1	0.2	0.3	0.4	0.5	0.7	1	1	2	3	5	7	10
5p1	1.33	1.44	1.53	1.62	1.69	1.81	1.95	1.94	2.25	2.44	2.65	2.77	2.89
5p0	1.09	1.22	1.33	1.43	1.51	1.65	1.81	1.81	2.15	2.35	2.57	2.70	2.81
5s	1.03	1.02	1.01	1.00	1.00	9.99_{-1}	9.99_{-1}	9.93_{-1}	1.01	1.02	1.04	1.06	1.08
4d2	1.17	1.32	1.40	1.47	1.53	1.62	1.74	1.73	2.03	2.26	2.61	2.88	3.20
4d1	9.14_{-1}	1.06	1.17	1.26	1.33	1.45	1.59	1.58	1.92	2.16	2.54	2.83	3.19
4d0	8.01_{-1}	9.48_{-1}	1.05	1.14	1.22	1.35	1.50	1.50	1.86	2.12	2.51	2.81	3.18
4p1	8.20_{-1}	9.22_{-1}	1.01	1.06	1.09	1.11	1.12	1.11	1.14	1.16	1.20	1.23	1.29
4p0	5.81_{-1}	6.80_{-1}	7.27_{-1}	7.64_{-1}	7.93_{-1}	8.32_{-1}	8.48_{-1}	8.52_{-1}	8.77_{-1}	9.02_{-1}	9.55_{-1}	1.00	1.07
4s	7.11_{-1}	7.86_{-1}	8.54_{-1}	9.02_{-1}	9.27_{-1}	9.42_{-1}	9.49_{-1}	9.64_{-1}	9.91_{-1}	1.02	1.07	1.11	1.17

The impact parameter moments $\left\langle b^1_{nlm} \right\rangle$ and $\left\langle b^{-1}_{nlm} \right\rangle$ are important values, specially to compare with classical trajectory Monte Carlo calculations. The classical microcanonical ensamble, usually used to describe the initial state velocity distribution, has a finite space dimension. It produces probabilities $P(b)$ that falls down abruptly with increasing impact parameter. Thus, total cross sections are generally well reproduced at expenses of an enhancement of the value at the origin, $P(b = 0)$. The comparison with the present ab initio results in two regions: $P(0)$ and $\left\langle b^1_{nlm} \right\rangle$ can shed some light on the reliability of the approach. For these reason in Tables 8–13 we display the CDW-EIS and first Born approximation values for the impact parameter moments of order −1 and +1 in the ionization of Ne, Ar, Kr and Xe, considering the different sub-shells and impact proton energies between 100 keV and 10 MeV.

6. Conclusions

In this contribution we present detailed *ab initio* results concerning the ionization processes of Ne, Ar, Kr, and Xe by proton impact. The inner-shell ionization cross sections are compared with the experimental data and with the ECPSSR predictions, when available. We tabulated the results of total cross sections, probabilities at zero impact parameter, and two impact parameter moments for ionization, using the CDW-EIS approximation for energies up to 1 MeV and the first Born approximation for higher

energies, up to 10 MeV. We have considered all the sub-shells of Ne and Ar, the L-M-N shells of Kr, and the M-N-O shells of Xe. In this way we have described the ionization processes through the corresponding cross sections for the different initial bound sub-shells and the ionization probability through four values: σ_{nlm}, $P_{nlm}(0)$, $\left\langle b_{nlm}^{1}\right\rangle$ and $\left\langle b_{nlm}^{-1}\right\rangle$. Imposing these four conditions to a reasonable trial expression for $P_{nlm}(\vec{b})$ one can describe most of the physics involved, even for multiple ionization processes.

Acknowledgements

The authors acknowledge the financial support from the following Argentine institutions: Consejo Nacional de Investigaciones Científicas y Técnicas (CONICET), Universidad de Buenos Aires, through the programme UBACyT, and Agencia Nacional de Promoción Científica y Tecnológica (ANPCyT).

References

[1] J. Miranda, G. Lapicki, At. Data Nucl. Data Tables 100 (2014) 651–780.
[2] S.A.E. Johansson, J.L. Campbell, K. Malmqvist (Eds.), Particle induced X-ray spectrometry (PIXE), John Wiley & Sons, New York, 1995.
[3] J. Ferraz Dias, L. Amaral, M.L. Yoneama (Eds.), Proceedings of the 13th International Conference on Particle Induced X-ray Emission (PIXE 2013), Nucl. Instrum. and Meth. Phys. Res. B 318 (2014) 1–218.
[4] M.G. Pia, G. Weidenspointner, M. Augelli, L. Quintieri, P. Saracco, M. Sudhakar, A. Zoglauer, IEEE Trans. Nucl. Sci. 56 (2009) 3614–3649;;
M.G. Pia, G. Weidenspointner, M. Augelli, L. Quintieri, P. Saracco, M. Sudhakar, A. Zoglauer, J. Phys. Conf. Ser. 219 (2010) 032018.
[5] R.E. Olson, J. Phys. B At. Mol. Phys. 12 (1979) 1843.
[6] T. Spranger, T. Kirchner, J. Phys. B At. Mol. Opt. Phys. 37 (2004) 4159.
[7] E.G. Cavalcanti, G.M. Sigaud, E.C. Montenegro, M.M. Sant 'Anna, H. Schmidt-Bocking, J. Phys. B At. Mol. Opt. Phys. 35 (2002) 3937.
[8] C.C. Montanari, E.C. Montenegro, J.E. Miraglia, J. Phys. B At. Mol. Opt. Phys. 43 (2010) 165201.
[9] C.C. Montanari, J.E. Miraglia, J. Phys. B At. Mol. Opt. Phys. 45 (2012) 105201.
[10] M.E. Galassi, R.D. Rivarola, P. D Fainstein, Phys. Rev. A 75 (2007) 052708.
[11] C.D. Archubi, C.C. Montanari, J.E. Miraglia, J. Phys. B At. Mol. Opt. Phys. 40 (2007) 943.
[12] C.C. Montanari, J.E. Miraglia, J. Phys. B At. Mol. Opt. Phys. 47 (2015) 105203.
[13] C.C. Montanari, J.E. Miraglia, J. Phys. B At. Mol. Opt. Phys. 48 (2014) 165203.
[14] H. Paul, Nucl. Instr. Meth. 192 (1982) 11–24, Also at http://www.exphys.jku.at/Kshells.
[15] H. Paul, J. Sacher, At. Data Nucl. Data Tables 42 (1989) 105.
[16] I. Orlic, C.H. Sow, S.M. Tang, At. Data Nucl. Data Tables 56 (1994) 159.
[17] W. Brandt, G. Lapicki, Phys. Rev. A 23 (1981) 1717.
[18] G. Lapicki, Nucl. Instr. Meth. Phys. Res. B 189 (2002) 820.
[19] G. Lapicki, Nucl. Instr. Meth. Phys. Res. B 318 (2014) 6–10.
[20] M. Pajek et al., Phys. Rev. A 73 (2006) 012709.
[21] D. Mitra, M. Sarkar, D. Bhattacharya, S. Santra, A.C. Mandal, G. Lapicki, Nucl. Instr. Meth. Phys. Res. B 268 (2010) 450.
[22] T. Mukoyama, Nucl. Instr. Meth. Phys. Res. B 354 (2015) 155–158.
[23] J.E. Miraglia, M.S. Gravielle, Phys. Rev. A 78 (2008) 052705.
[24] J.E. Miraglia, Phys. Rev. A 79 (2009) 022708.
[25] A.C. Tavares, C.C. Montanari, J.E. Miraglia, G.M. Sigaud, J. Phys. B At. Mol. Opt. Phys. 47 (2014) 045201.
[26] D.S.F. Crothers, J.F. McCann, J. Phys. B 16 (1983) 3229.
[27] P.D. Fainstein, V.H. Ponce, R.D. Rivarola, J. Phys. B At. Mol. Opt. Phys. 21 (1988) 287–299.
[28] R.D. Rivarola, P.D. Fainstein, V.H. Ponce, in: A. Dalgarno et al. (Eds.), Proc. 16th ICPEAC, AIP, New York, 1989.
[29] F. Salvat, J.M. Fernandez-Varea, W. Williamson Jr., Comput. Phys. Commun. 90 (1995) 151.
[30] S.J. Cipolla, Comput. Phys. Commun. 182 (2011) 2439–2440;;
S.J. Cipolla, Comput. Phys. Commun. 184 (2013) 2230–2231.
[31] Z. Smit, G. Lapicki, J. Phys. B At. Mol. Opt. Phys. 47 (2014) 055203.
[32] M. Rodbro, E. Horsdal Pedersen, C.L. Cocke, J.R. Macdonald, Phys. Rev. A 19 (1979) 1936.
[33] C.L. Cocke, R.K. Gardner, B. Curnutte, T. Bratton, T.K. Saylor, Phys. Rev. A 16 (1977) 2248.
[34] J.E. Golden, J.H. McGuire, Phys. Rev. A 15 (1977) 499.
[35] N. Stolterfoht, D. Schneider, Phys. Rev. A 11 (1975) 721.
[36] L.M. Winters, J.R. Macdonald, M.D. Brown, L.D. Ellsworth, T. Chiao, Phys. Rev. A 7 (1973) 1276.
[37] S.J. Czuchlewski, J.R. Macdonald, L.D. Ellsworth, Phys. Rev. A 11 (1975) 1108.
[38] W.M. Ariyasinghe, H.T. Awuku, D. Powers, Phys. Rev. A 42 (1990) 3819–3825.
[39] G. Schiwietz, U. Stettner, T.J.M. Zouros, N. Stolterfoht, Phys. Rev. A 35 (1987) 598.
[40] N. Maeda, N. Kobayashi, H. Hori, M. Sakisaka, J. Phys. Soc. Jpn. 40 (1976) 1430.
[41] N. Stolterfoht, D. Schneider, P. Ziem, Phys. Rev. A 10 (1974) 81.
[42] M.E. Rudd, Phys. Rev. A 10 (1974) 518.
[43] J.B. Crooks, M.E. Rudd, Phys. Rev. A 3 (1971) 1628.
[44] R.L. Watson, L.H. Toburen, Phys. Rev. A 7 (1973) 1853.